

Nanoscale

Accepted Manuscript

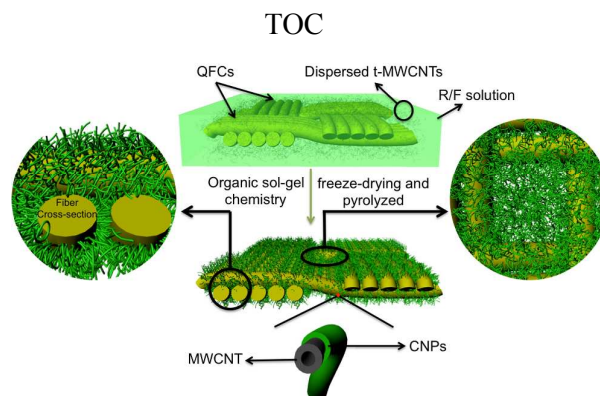


This is an *Accepted Manuscript*, which has been through the Royal Society of Chemistry peer review process and has been accepted for publication.

Accepted Manuscripts are published online shortly after acceptance, before technical editing, formatting and proof reading. Using this free service, authors can make their results available to the community, in citable form, before we publish the edited article. We will replace this *Accepted Manuscript* with the edited and formatted *Advance Article* as soon as it is available.

You can find more information about *Accepted Manuscripts* in the [Information for Authors](#).

Please note that technical editing may introduce minor changes to the text and/or graphics, which may alter content. The journal's standard [Terms & Conditions](#) and the [Ethical guidelines](#) still apply. In no event shall the Royal Society of Chemistry be held responsible for any errors or omissions in this *Accepted Manuscript* or any consequences arising from the use of any information it contains.



The electrical conductivity of quartz fiber cloths (QFCs)/MWCNT-carbon aerogel (MCA)/PDMS (QMCA/PDMS) composite is very high at low nanotubes loading, which remains constant after many times of bending and exhibits an increase of $\sim 170\%$ than that of MCA/PDMS at 20% strain. Attributing to the synergistic effects of optimized MWCNTs network and fortifier QFCs in composite, the tensile strength, modulus and electromagnetic interference shielding effectiveness of QMCA/PDMS laminate are also excellent. Therefore, this brand-new flexible conductive material can meet the demands of next-generation electronics while also protect them against harms from external forces and EMI.

Cite this: DOI: 10.1039/c0xx00000x

www.rsc.org/xxxxxx

ARTICLE TYPE

Highly conductive and flexible polymer composites with improved mechanical and electromagnetic interference shielding performances

Mengting Chen, Ling Zhang* Shasha Duan, Shilong Jing, Hao Jiang, Meifang Luo and Chunzhong Li*

Received (in XXX, XXX) Xth XXXXXXXXXX 20XX, Accepted Xth XXXXXXXXXX 20XX

DOI: 10.1039/b000000x

New flexible and conductive materials (FCMs) comprising quartz fiber cloths (QFCs) reinforced multi-walled carbon nanotubes (MWCNTs)-carbon aerogel (QMCA) and poly(dimethylsiloxane) (PDMS) have been successfully prepared. The QMCA/PDMS composite with a very low loading of MWCNTs (~ 1.6 wt%) demonstrate enhanced performances in tensile strength (129.6 MPa), modulus (3.41 GPa) and electromagnetic interference (EMI) shielding efficiency (SE) (~ 16 dB in X-band (8.2-12.4 GHz) region). Compared to QC (MWCNTs were simply deposited on the QFCs without forming aerogel networks) based PDMS composite, a ~ 120%, 330% and 178% increase is obtained, respectively. Moreover, the EMI SE of QMCA/PDMS composite can further reach 20 dB (a SE level needed for commercial applications) with only 2 wt% MWCNTs. On the other hand, the conductivity of QMCA/PDMS laminate can reach 1.67 S cm^{-1} even with such low MWCNTs (1.6 wt%), which still remains constant even after 5000 times bending and exhibits an increase of ~ 170% than that of MWCNT-carbon aerogel (MCA)/PDMS at 20% strain. Such intriguing performances are mainly attributed to their unique networks in QMCA/PDMS composites. In addition, these features can also protect electronics against harms from external forces and EMI, making the brand-new FCMs a huge potential in next-generation devices, like E-skin, robot joints and so on.

Introduction

For the past decades, flexible and conductive materials (FCMs) have changed the ways of application – to transport electron with flexible pathway and soften digital equipment.¹⁻⁶ Such interesting potential has attracted increasing attention,⁷ one of the most popular strategy that has been developed in recent years is to combine diverse active and passive electronic components with elastomer polymer. Carbon nanotubes (CNTs) with extremely high electrical property, for instance, is a common choice to establish an electrical pathway in elastomer matrix. The combination of CNTs and elastomer is showing great promise to be ideal candidate for building FCMs.

However, in some easily commercialized ways, e.g. high-shear or ultrasonically mixing,^{3,8} CNTs are easy to agglomerate in the matrix due to high aspect ratio and strong π - π interactions between them⁷, and thus the conductive network they formed usually leaves too much to be desired. As a consequence, good electrical pathway ($> 1 \text{ S/cm}$) could only be built with high CNTs concentration ($> 10 \text{ wt\%}$).⁸⁻¹¹ Shimizu *et al.*³ fabricated multi-walled carbon nanotubes (MWCNTs)/poly[styrene-*b*-(ethylene-co-butylene)-*b*-styrene] (SEBS) composite with an electrical conductivity of about 0.2 S/cm at 5.5 wt% MWCNTs loading. While CNT/Nafion composite film made by Luo *et al.*¹⁰ reached a high electrical conductivity of above 15 S/cm with 52 wt% CNT loading. The awful distribution and dispersion of MWCNTs

leads to inferior conductive network, which has negative effect on the conductivity of composites. To overcome this limitation, MWCNTs carbon aerogel (MCA), a preformed highly porous three-dimensional (3D) superior network composed of MWCNTs, is reckoned to solve all the aggregation problems.¹² Then, by infiltrating this unique electric network with elastomer matrices, like poly(dimethylsiloxane) (PDMS), the composite shows high electrical conductivity with very low CNTs loading.¹³

In addition to outstanding electrical performance, great structural strength and electromagnetic interference (EMI) shielding are another two attractive properties for applications in engines, machinery, aircraft/aerospace and next-generation FCMs, such as portable devices, E-skin and robot joints.¹⁴⁻¹⁶ High strength broadens the durability and applications of the composites. While, the EMI shielding performance endows FCMs with resistance to electromagnetic radiation produced from modern electronic. That is very beneficial for human body, environment and especially the precision electronic equipment today and in the future.^{17, 18} In EMI field, it is believed that fiber composites are supposed to be the ideal substitution of traditional metallic materials only if their inherent electromagnetic shielding capabilities were improved.¹⁸ C. J. von Klemperer and D. Maharaj combined fabrics with metal powders to manufacture fiber cloths (FCs)-reinforced polymer composites, which revealed excellent EMI shielding effectiveness (SE). Furthermore, FCs-reinforced FCMs can also provide high stiffness and strength with low density, expanding the possibilities of applications in

areas like aircraft/aerospace industry. In general, the FCs-FCMs are desired choice for forthcoming flexible electronics, robot joints for example, which are also requiring high strength and excellent EMI shielding performance for protection.

Hence, in this paper, we've presented a composite structure combining 3D optimized MCA conductive network with 2D fortifier quartz fiber cloths (QFCs), which we called as QMCA. The special-designed QMCA has superior conductive pathway and more robust structure than QC (MWCNTs were simply covering on the QFCs without forming 3D aerogel networks) preform. When infiltrated QMCA with PDMS, this new kind FCMs exhibited very high conductivity, outstanding strength and commendable EMI shielding performance simultaneously. After mechanical test, the tensile strength and modulus of QMCA/PDMS film are 129.6 MPa and 3.41 GP respectively, showing a ~ 120 % and 330 % increase against QC/PDMS laminate. Furthermore, attributing to the optimized connectivity of MWCNTs, EMI SE of QMCA/PDMS exhibits a ~ 178% increase. The nanotubes superior connectivity also gives QMCA/PDMS composite a very high electrical conductivity, 1.67 S cm⁻¹, with only 1.6 wt% MWCNTs loading, as it costs QC/PDMS about 13.5 wt% to reach the same value. The electrical conductivity of QMCA/PDMS remains constant even after 5000 times bending, and exhibits an increase of ~ 170% than that of MCA/PDMS at 20% strain (1.67 S cm⁻¹, 1.6 wt% MWCNTs loading). In brief, a brand new composite structure (QMCA/PDMS) has been developed, the combination of QFCs and MCA maximized the advantages of both materials, providing a remarkably increase in mechanical and EMI shielding performances of FCMs while retaining their conductivities almost completely. These outstanding properties can successfully broaden the applications of FCMs to a great extent.

Experimental

Commercially available QFCs (~ 5 μm in diameter) with high heat resistance were used for this work. Quartz fiber is an advanced material that can withstand very high temperature. Pristine MWCNTs synthesized by chemical vapor deposition process (purity: about 95%, diameter: 10-20 nm, length: 5-20 μm) were purchased from Chengdu Organic Chemicals Co., Ltd., Chinese Academy of Sciences, China. Resorcinol (R, purity with 99%) and formaldehyde solution (F, 36.5% in water) were purchased from Aladdin Chemistry Co., Ltd., Shanghai, China. Poly(dimethylsiloxane) (PDMS) prepolymer was prepared by mixing base silicone gel (Sylgard 184, Dow Corning) with a curing agent (Sylgard 184 silicone elastomers curing agent) in a 10:1 weight ratio. Sulfuric acid (H₂SO₄, 95%), nitric acid (HNO₃, 60%) and sodium carbonate (Na₂CO₃, 99%) were obtained from Shanghai Lingfeng Chemical Reagent Co., Ltd., China. All reagents were analytical purity and used as received.

50 Fabrication of QMCA and its composite.

The QFC/t-MWCNT-carbon aerogels were prepared using traditional organic sol-gel chemistry method as we mentioned in previous work.¹² The preparation process is shown in Scheme 1. Briefly, t-MWCNTs (MWCNTs with mixed acid treatment, 0.5 wt% in the reaction mixture) were suspended in DI (deionized water) and dispersed using ultrasonic cell disruptor (model JY96-

II, sonic power ~ 150 W, frequency ~ 20 kHz, Ningbo Haishu Kesheng Ultrasonic Equipment Co., Ltd., Ningbo, China) for 2h. When the time was up, resorcinol (R, 0.247 g, 2.24 mmol), formaldehyde solution (F, 0.357 g, 4.41 mmol) and catalyst Na₂CO₃ (1.19 mg, 0.011 mmol) were added to the reaction solution. Then the fiber cloth was cut into pieces of 40 mm × 30 mm, here we took two pieces of QFCs and dipped them into the reaction solution mentioned above. The polycondensation reaction between R and F under alkaline conditions produces surface functionalized polymer "Clusters", which will coat on uniformly dispersed MWCNTs and can be crosslinked in gels with 3D network. The starting concentration of R and F in the mixture was 3.58 wt%, the molar ratio of R:F and R:C was 1:2 and 200:1, respectively. It is reported that this proportion among the R, F and C is optimal for the performance of RF aerogels.²⁰ After 2 hours of ultrasonic mixing, the mixture solutions were cured in petri dish at 85 °C for 72 h to form organic gels, which were then immersed into water for another 48 h to remove small RF molecules. Freeze-drying was used to dry the t-MWCNT/QFC organic gels, afterwards the dried gels were pyrolyzed at 1000 °C under inert atmosphere and thus the t-MWCNT/QFC-carbon aerogels were obtained.

The PDMS prepolymer was prepared by mixing base silicon gel with curing agent in a weight ratio of 10:1. Then these aerogels were backfilled with PDMS prepolymer using vacuum suction method we mentioned in previous work²¹ and cured at 90 °C for 30 min. These final aerogels/PDMS composites had approximately the same dimensions as the original aerogels.

55 Preparation of MCA/PDMS and QC/PDMS Composites.

The MCA/PDMS films were prepared as we mentioned in previous work.¹² The QC/PDMS films can be fabricated very simple. Briefly, t-MWCNTs (0.5 mg ml⁻¹) were suspended in DI and dispersed using ultrasonic cell disruptor for 2h, then, two pieces of fiber cloths (40 mm × 30 mm) were directly dipped into the solution. After dried in oven at 60 °C, the white QFCs changed into black, meaning the nanotubes were adhered onto quartz fibers. Then, the dried QFC/MWCNT (QC) preforms were backfilled with PDMS prepolymer using vacuum suction method and cured at 90 °C for 30 min to get QC/PDMS composites.

Characterization.

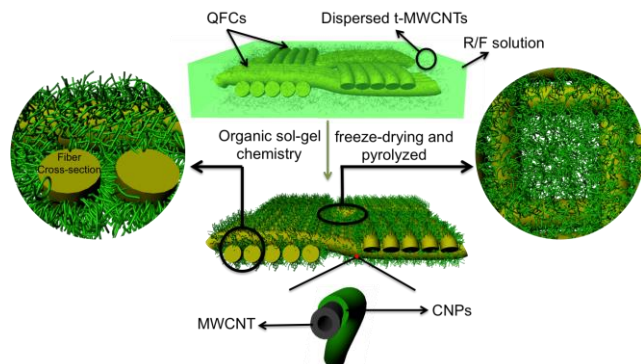
The morphology of QMCA and the fibers-graphitic materials-matrix adhesion of QMCA/PDMS composite films were examined by using a field emission scanning electron microscopy (FE-SEM, Hitachi S-4800), operating at 5kV. The electrical conductivity of QMCA/PDMS composite film was measured by four-point probes (model RTS-8, Guangzhou 4Probes Tech Industrial Co., Ltd., Guangzhou, China) contact direct current (dc) conductivity measurement method at room temperature. The tensile tests were performed using a universal testing machine (CMT4204, Sansi Co., Ltd, China). The electromagnetic interference shielding effectiveness (EMI SE) was measured in the X-band frequency of 8.2-12.4 GHz using an Agilent N5242A PNA-X Microwave Network Analyzer. The composites were cut into 22.86 mm × 10.16 mm pieces for measurements.

Results and discussion

Here, in our study, we've fabricated three kinds of composites, they are MCA/PDMS, QMCA/PDMS and QC/PDMS laminates, respectively.

Laminates Fabrication and Their Mechanical Properties.

As for fabrication of QMCA preform, the water-soluble organics (R and F) are the only but crucial difference from QC preform preparation. As illustrated in Scheme 1, through organic sol-gel chemical reaction and annealing at 1000 °C under Ar atmosphere, the cross-linked organic precursor (R/F) completely transforms into carbon nano-particles (CNPs). The CNPs wrap on nanotubes, fibers and nanotube-fiber junctions uniformly, forming t-MWCNTs carbon aerogel throughout the cloths.



Scheme 1. Schematic illustration of QMCA preparation.

The microstructure of QMCA is special-designed, as shown in Fig. 1, which is striking contrast to QC preform. The MWCNTs in QMCA are uniformly dispersed without any aggregation (inset of Fig. 1a); and the long-distance link of 3D conductive networks not only covers the vertical-connected fibers tightly in Fig. 1a (red dotted lines), but also steps over the clearance and connecting adjacent fibers together (Fig. 1b), endowing the QMCA with excellent conductive pathway all over the cloth. As for the QC preform, after undertaking a drastic contraction during evaporation of solvent, the MWCNTs deposited on fibers present a highly entangled morphology with local aggregation (red circles in Fig. 1c). Moreover, the nanotubes just stack together instead of building any long-distance links or networks between adjacent fibers (Fig. 1d). These disconnections among fibers limit electrons transport between them. Therefore, QMCA has a superior conductive structure than QC preform, and that makes its polymer composite attracts wider attentions.

The better morphology of nanotubes and fibers in QMCA is mostly attributed to the unique CNPs introduced from R/F. The CNPs have played two roles during the whole process: First, the R/F polymerized so homogeneously that even single nanotube has been coated with CNPs uniformly (inset of Fig. 1b), which helps MWCNTs form a highly porous 3D conductive network throughout cloths. The second role of CNPs is reinforcement. The CNPs are considered as "binder",^{12, 13} which can not only improve the contact between adjacent nanotubes (as shown in Fig. S2, ESI), resulting in high electrical conductivity of 1.67 S cm⁻¹ in QMCA/PDMS; but also enhance the connections between MWCNTs network and QFCs (Fig. 1a, b), increasing the tensile strength and modulus of the composite to 129.6 MPa and 3.41 GPa. That's to say, the CNPs assist QMCA in gaining multiple

structural advances contrast against QC preform, and endow QMCA/PDMS composite with various excellent performances in following tests.

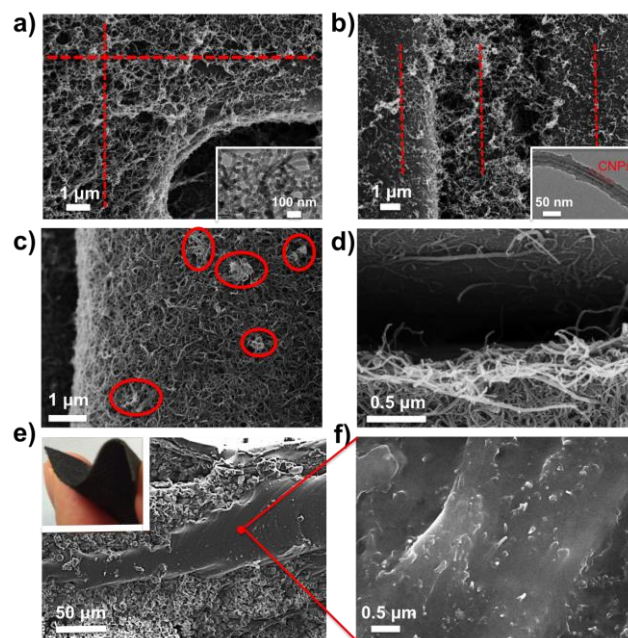


Fig. 1. FE-SEM images of QMCA (a and b) and QC (c and d) preforms, the inset of (a) and (b) are FE-TEM images of the nanotubes network on fiber cloths and single MWCNT in aerogel structure, respectively. Red lines in (a) and (b) represent axis direction of fibers, red circles in (c) exhibit aggregation of MWCNTs. (e) and (f) are FE-SEM images of QMCA/PDMS laminate, the inset of (e) is the photographs of it.

Then, the porous QMCA preform was completely infiltrated with PDMS by vacuum-assisted suction method, and its fracture surface was examined by FE-SEM. The QMCA/PDMS laminate can be bended arbitrarily (inset of Fig. 1e). Fig. 1e shows that the fibers are all surrounded and well impregnated with polymer, indicative of good wetting and fiber-matrix interfacial adhesion.²⁰ Meanwhile, a matrix-rich region existing between two quartz plies contains distinct MWCNTs inside (Fig. 1f), which declares that the nanotubes networks also covered spaces between cloths, connecting isolated fibers into an integrity. Owing to the unique structure of QMCA and its compact adhesive to PDMS, the QMCA/PDMS composites are expected to show high mechanical performances.

The mechanical properties of MCA/PDMS, QFC/PDMS, QC/PDMS and QMCA/PDMS laminates are all investigated using tensile stress vs. strains measurements (Fig. 2). After integrating QFCs and MCA tightly, the QMCA/PDMS composite has excellent mechanical properties. The tensile strength and modulus of it can separately reach 129.6 MPa and 3.41 GPa. These values are not only far larger than the simple sum of QFC/PDMS and MCA/PDMS laminates, but also show a ~ 120% and ~ 330% increase than QC/PDMS composite (108.3 MPa and 1.03 GPa), respectively (shown in Fig. 2b).

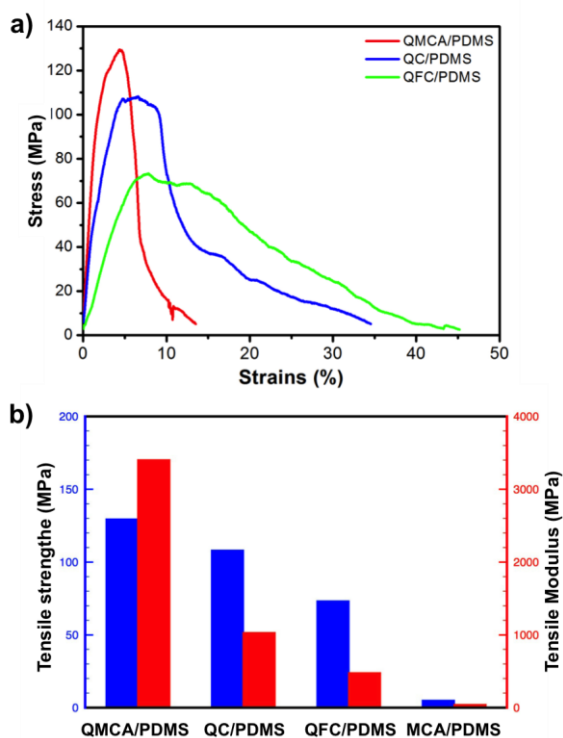


Fig. 2 Mechanical properties of these laminates: (a) stress curves of QMCA/PDMS, QC/PDMS and QFC/PDMS laminates as a function of strains; (b) the tensile strength and modulus of QMCA/PDMS, QC/PDMS, QFC/PDMS and MCA/PDMS composites, respectively.

In order to further analysis the outstanding mechanical performances of QMCA/PDMS composite, the fracture surfaces of QFC/PDMS, QC/PDMS and QMCA/PDMS laminates after extension test have all been examined by FE-SEM (Fig. 3). For QFCs reinforced PDMS composites, the fibers expose clean and smooth surfaces (Fig. 3a and b), indicating the bonding between fiber/matrix is so weak that fibers can be pulled out from matrix very easily, and thus the load applied cannot be effectively transferred to the fortifier. Conversely, in QC/PDMS and QMCA/PDMS laminates, the nanotubes coating lead to increased roughness of quartz fibers surfaces^{22, 23} and stronger interfacial bonding at fiber/PDMS interface. Hence, after investigated by extension test, chunks of polymer residue still adhere on fibers surfaces (Fig. 3d and f), indicating the improved interaction between fiber/matrix. That is to say, nanotubes help both QC/PDMS and QMCA/PDMS laminates show much better mechanical properties than QFC/PDMS composite.

Nonetheless, the different nanofillers morphology in QMCA/PDMS and QC/PDMS laminates is another important factor affecting the mechanical performances of them. In contrast to the entangled and aggregated MWCNTs in QC preform (Fig. 1c, d), the consecutive nanotubes network in QMCA shows a high porous structure (Fig. 1a, b). These 3D CNT networks, acting as fishing net, hook the whole QFCs completely and support vast channels for PDMS to pass through and bond with fibers directly, which suggests better interaction between the fibers and matrix in QMCA/PDMS composite. The residue layer on fibers in QMCA/PDMS is quite rough compared to that in QC/PDMS (Fig. 3 d and f), further demonstrating a more tight connection between matrix and cloths. While in QC/PDMS, the

delamination between matrix and fibers can be observed in the red circles in Fig. 3c and inset of Fig. 3d. As a consequence, the structure of QMCA/PDMS composite is more stable than QC/PDMS composites and needs more energy for the structure to fail. As shown in Fig. 2a, when the same tension forces were applied to these laminates, QMCA/PDMS composites would exhibit the smallest strain, equal to the conclusion that QMCA/PDMS laminate possesses the largest tensile modulus. Therefore, combination of QFCs and nanotubes aerogel network endows QMCA/PDMS composite the best mechanical properties.

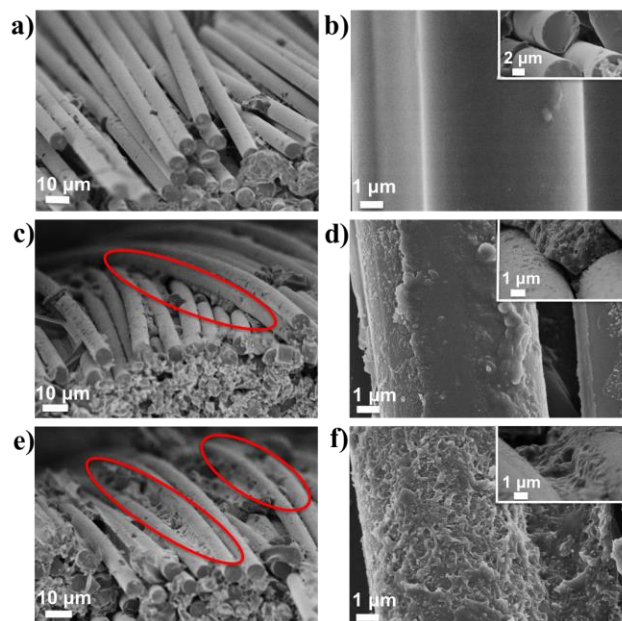


Fig. 3 FE-SEM images of composites after tensile test: (a) smooth surface of neat quartz fibers without CNTs and their magnified images (b) and inset in (b); with the addition of MWCNTs, fibers in (c) QC and (e) QMCA all show more rough surfaces; furthermore, magnified image of QC (d) shows less polymer sticks to the surface of fibers, and its inset image illustrates delamination between matrix and fibers; while magnified image of QMCA (f) exhibits uniformly coating of polymer on fibers surfaces, and its inset image shows matrix bridged adjacent fibers.

The Electrical Conductivities of QMCA/PDMS Laminate.

Owing to the unique and superior synergistic carbon nanotubes-carbon aerogels/quartz fiber cloths structure in QMCA, the QMCA/PDMS laminate not only exhibits the best mechanical properties, but also shows an exceptional electrical performance. Fig. 4a shows the conductivity for QMCA/PDMS laminates as a function of MWCNTs concentration. It is obvious that an abruptly increased conductivity can be observed at 0.1 wt% (0.13 S cm⁻¹) MWCNTs loading, indicating the percolation threshold for QMCA/PDMS is much smaller than for QC/PDMS (0.5 wt% MWCNTs, 1 × 10⁻³ S cm⁻¹, Fig. S3, ESI). The result can be attributed to the action of CNPs. During the condensation polymerization process, the uniformly dispersed MWCNTs were fixed with each other and adhered onto the fibers by cross-linked RF, then formed a superior network overall the QFCs. Subsequently, the insulating polymer coating RF have been further carbonized into CNPs. Therefore, compared to the percolating network in QC/PDMS with local aggregate

MWCNTs (due to the large Van der Waals forces among nanotubes) and large gap between fibers (Fig. 1), better conductive network would be constructed more efficiently with less nanotubes and covered the whole QMCA/PDMS. Simultaneously, the CNPs act as “binder” to coat on the adjacent MWCNTs and improve the contacts between the nanotubes significantly, enhancing the electrons transportation further on. As a consequence, much higher conductivity has shown in QMCA/PDMS laminate with lower percolation threshold compare with QC/PDMS.

Conductivities of QMCA/PDMS increased as a function of MWCNTs concentrations above percolation threshold, reaching 1.67 S cm^{-1} with only 1.6 wt% MWCNTs loading. This value is almost two orders of magnitude higher than QC/PDMS with same MWCNTs loading ($1 \times 10^{-2} \text{ S cm}^{-1}$, 1.6 wt% MWCNTs). This is attributed to the special-designed 3D MWCNTs network in QMCA, which helps to provide a superior pathway for electrons transportation. Since the aerogel structure is the key factor affecting conductivity, here we only contrast the QMCA/PDMS with MCA/PDMS composites, to explore the advantages when QFCs combining with nanotubes networks.

Flexible conductors demand that the composites have the capacity to absorb large levels of strain ($\gg 1\%$) without fracture, or repeatedly cycling of a certain stress won't cause significantly degradation in their electrical properties.²⁴ Therefore, the electrical conductivity retention capability of QMCA/PDMS laminate under tensile strains (within the range of 0% to 20%) and cyclic bending tests were chosen to measure the performances of samples (Fig. 4b and c). The recorded values are normalized by the sample initial conductivity σ_0 at zero strain (σ/σ_0) as a function of the applied tensile strain. Though the QFC is made of orthotropic quartz fibers with a very high shear modulus, fibers still can move more freely in the diagonal direction,²⁵ thus, the composite laminates have been stretched along 45 degree angle instead of fibers' directions, which could be the most effective way to observe changes during the tests. Obviously, the electrical conductivities of QMCA/PDMS and MCA/PDMS laminates both decreased as the tensile strain increased from 0 % to 20% (Fig. 4b). The main reason for this phenomenon can be attributed to the structure-change during the stretch procedure. Once the tension force applied to the preformed MWCNTs conductive network, the uniform but randomly oriented nanotubes are forced to align along the stretching direction³ by stress, and thus slippages occurred between interconnected nanofillers,¹² resulting in partial damage of network and decrease of conductivity. However, in comparison between QMCA/PDMS and MCA/PDMS laminates, the former lost 50% in σ/σ_0 while the latter dropped 70% at the same strain, which means the electrical conductivity retention rate of QMCA/PDMS laminate is nearly 1.7 \times higher than that of MCA/PDMS at 20% strain. The cooperation of MWCNTs aerogel and QFCs in QMCA/PDMS laminate helps to contribute this result. First, the high strength orthotropic fibers shared the deformation greatly; Secondly, the reinforcing CNPs not only cover and strengthen the MWCNTs network itself, but also connect the networks with fibers where the stress could be transmitted to, remitting the damage of network and keeping the conductivity pathway stable. Therefore, with the synergy between

QFCs and nanotubes network, the QMCA/PDMS composites show greatly improved electrical properties than MCA/PDMS does.

To further investigate the electrical property of QMCA/PDMS laminate under mechanical deformation, the conductivity of composite was also measured during bending from 0° to 180° repeatedly for thousands of times. Fig. 3c illustrates that the conductivity exhibits little change even after 5000 times bending. So we can conclude that the composite laminate reveals little sensitivity to cyclic bending deformation, which is because the 3D MWCNT network in the flexible PDMS matrix can effectively buffer bending deformation and hold the MWCNTs network almost integrated. The excellent conductivity of the stretchable conductors means that they can cover arbitrary curved surfaces²⁶ and work well in applications that demand bending durable.

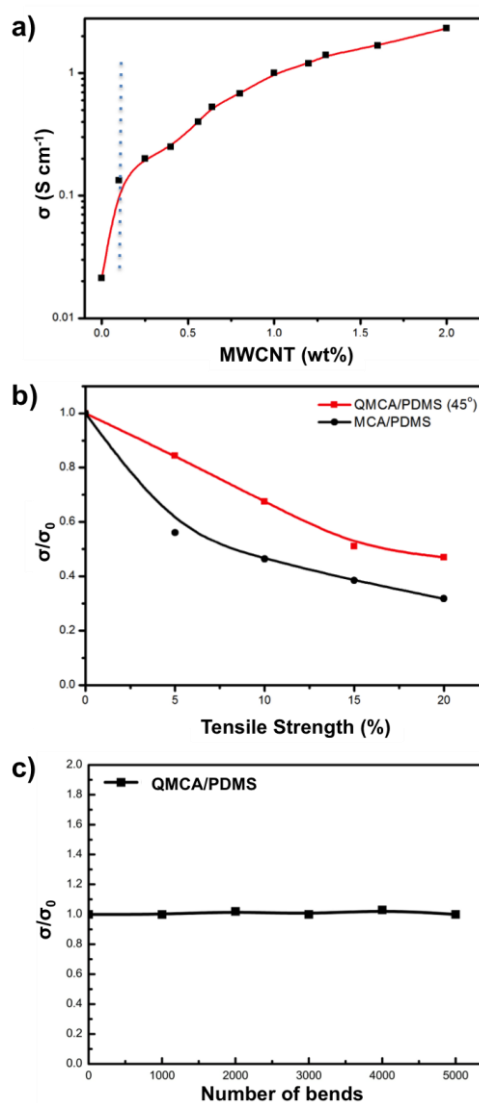


Fig. 4 (a) Conductivity of QMCA/PDMS composite with MWCNTs loading. Normalized conductivity of (b) the QMCA/PDMS and MCA/PDMS composite films as a function of tensile strain, and (c) QMCA/PDMS laminate as a function of the number of bends.

80 **EMI shielding effectiveness (SE)**

The severe electromagnetic radiation produced from modern electronics could be very harmful to precision electronic equipment, human body and environment.^{15,27} This is defined as electromagnetic interference (EMI), and should be blocked by using a conductive shield.¹⁷ For electrically conductive polymer nanocomposites, the EMI SE strongly relies on aspect ratio, conductivity, dispersion and fraction of conductive fillers in polymer.^{27, 28} Hence, the QMCA/PDMS laminates with outstanding electrical and mechanical properties are invested in high expectation on EMI shielding performance.

The electromagnetic wave contains magnetic field and electric field, these two components perpendicular each other and changes periodically. The EMI SE is defined as the logarithmic ratio of incoming (P_i) to transmitted power (P_t) of radiation and is expressed in decibels (dB). Reflection, absorption and multiple-reflection are three mechanisms of EMI SE, thus the total EMI SE is the sum of the effectiveness of reflection (SE_R), absorption (SE_A) and multiple-reflection (SE_M), which can be expressed in the following equations:

$$SE = -10\lg(P_t/P_i) = SE_A + SE_R + SE_M$$

$$SE_R = -10\lg(1-R)$$

$$SE_A = -10\lg[T/(1-R)]$$

Where R is the coefficient of reflectivity and T is the coefficient of transmissivity.

The multiple-reflections represent the reflections at various surfaces or interfaces within the shield. It should be noted that unlike the positive effect of reflection and absorption on EMI shielding, the multiple-reflection decreases the overall EMI SE. But when thickness of shield is larger than the skin depth, which is the distance that the wave strength decreases to e^{-1} ($e = 2.718$) of its incoming value in the shield interior, the multiple-reflection can be neglected.¹⁷ In this situation, when an electromagnetic wave strikes the shielding material, the exterior mobile charge carriers and interior electric/magnetic dipoles from the shield would interact with the wave to reflect them back²⁹ and attenuate them through absorption, respectively. According to the formulas mentioned by *M. H. Al-Saleh et. al.*³⁰, the reflection loss and absorption loss are functions of the ratio σ/μ and the product $\sigma\mu$, respectively. Where σ is the electrical conductivity and μ is the magnetic permeability. Thus, both SE_A and SE_R increase with increase in shielding conductivity. That is to say that enhanced connectivity of conductive fillers in shield, which means an elevated electrical conductivity, is believed to improve the EMI shielding performances of materials.^{31,32}

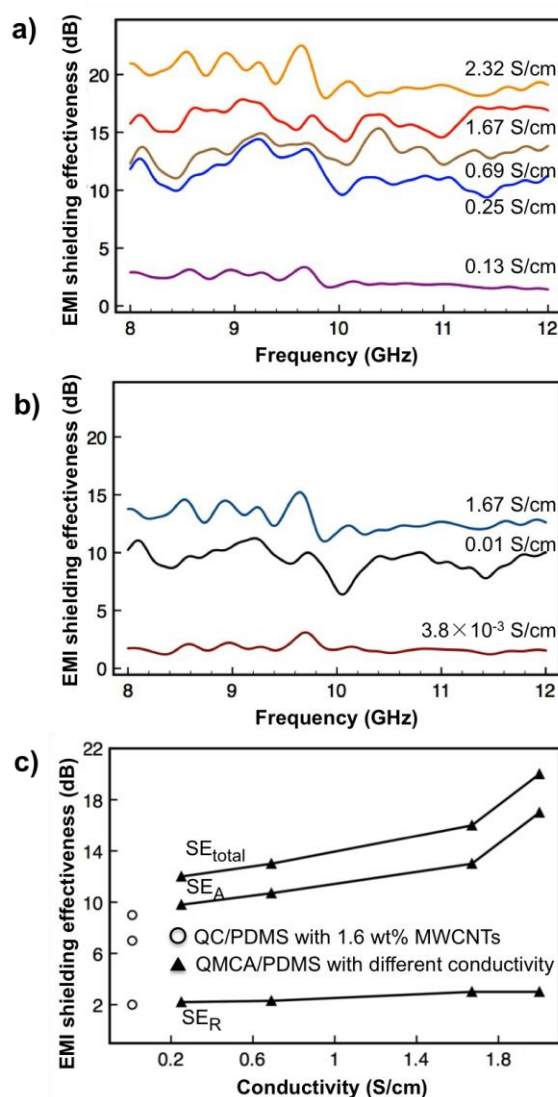


Fig. 5 EMI SE of (a) QMCA/PDMS and (b) QC/PDMS composites with different electrical conductivities measured in frequency range of 8-12 GHz; (c) SE_{total} , SE_A and SE_R of QMCA/PDMS with different electrical conductivities and QC/PDMS with 1.6 wt% MWCNTs at a frequency of 50 GHz.

Figure 5a and b shows the EMI SE of QMCA/PDMS and QC/PDMS laminates are measured in the X-band frequency ranges. The irregular EMI SE curves of all the composites fluctuate with frequency of incoming rays, which means the conductive networks of MWCNTs in both QMCA/PDMS and QC/PDMS laminates are also irregular.^{33,34} It is observed that the EMI SE of both QMCA/PDMS and QC/PDMS laminates increases with increased nanotubes concentration. The EMI SE of QMCA/PDMS increased from 3 dB to 16 dB with increasing MWCNTs loading from 0.1 wt% to 1.6 wt%, and reaching 20 dB (a SE level needed for commercial applications) with only ~ 2 wt% MWCNTs. While the SE of 0.7 wt% to 2 wt% nanotubes in QC/PDMS composite enhanced from 2 dB to 13 dB. The incremental in EMI SE of both composites can be attributed to the higher amount of free electrons in composites that can interact with the penetrating radiation,^{28, 35} leading a higher SE value. Secondly, at the same MWCNTs loading (1.6 wt%), the SE of

QC/PDMS composite is measured to be only ~ 9 dB over X-band, while the QMCA/PDMS laminate exhibits both a much higher conductivity of 1.67 S/cm and a significantly improved SE of ~ 16 dB (red curve in Fig. 5a). It is worth noting that same MWCNTs concentrations meant same amount of mobile charge carriers. Although shielding has no scientific relation with connectivity, it is increased by connectivity.³⁶ Therefore, the much higher EMI shielding performance of QMCA/PDMS is ascribed to the enhanced connectivity of conducting nanofillers in QMCA than in QC.

Fig. 5c shows the SE_R , SE_A and total SE (SE_{total}) of these two kinds laminates with different nanotubes concentrations at 9 GHz. For QMCA/PDMS composites (solid black triangle), both the SE_{total} and SE_A increase notably while electrical conductivity increasing, whereas the SE_R increases slightly. It is calculated that the shielding by absorption share of the total shielding increased from 79% to 85% with increasing the MWCNTs loading from 0.4 wt% to 2 wt%. And for QC/PDMS (hollow black circle), the SE_A percentage of SE_{total} is 78%. Therefore, we considered that for these MWCNTs composites most of the attenuation is due to absorption.

The shielding by absorption mechanism was further elucidated. The penetrating radiation would induce conduction and displacement currents inside the material. Conduction current is resulting from the directional movement of free electrons, which can provides electric loss. The increasing nanotubes concentrations in polymer equal to larger number of free electrons, then the conduction current is enhanced and more mobile charge carriers can attenuate the penetrating wave. While the displacement current associate with the real permittivity and produced from the localized charges, polarization for example. It is reported that at X-band frequency range, polarization of nanotubes and polymer in MWCNT-based composite can produce high real permittivity, which could contributes to increasing the shielding by absorption.¹⁷ The larger amount of nanotubes will build more intensive conductive networks and decreased gap distance between MWCNTs in matrix. Thus, the enhanced electric field on insulating matrix develops increased polarization of polymer, enhanced chance for electrons to pass the barriers (internal field emission, including tunnelling mechanism, which would occur when the distance between MWCNTs less than 10 nm in nanotubes composite.)^{28, 37} and improved SE_A . The increased MWCNTs concentration also means enhanced conductivity (Fig. 4a), hence, it can be concluded from the explanation and the equation mentioned above that the shielding by absorption is increasing with increase in conductivity.

Since the shielding by absorption is the principle influence factor for SE_{total} and increasing with conductivity. Therefore, for QMCA/PDMS (1.6 wt%, 1.67 S cm⁻¹) with the same nanofillers loading but much higher conductivity than QC/PDMS laminates (1.6 wt%, 0.01 S cm⁻¹), the SE_A reaches as high as ~ 13 dB, almost 2× larger than the latter composite (~ 7 dB). This phenomenon associates with the better structure of QMCA than QC. In QMCA preform, the conductive network and connectivity of nanofillers are both superior and the barriers between MWCNTs are narrower than in QC for electrons crossing. Thus, the higher conductivity endows QMCA/PDMS with better

performance in absorption than QC/PDMS composite.

Therefore, the QMCA/PDMS laminates are more suitable than QC/PDMS composites in robust and flexible EMI shielding applications.

Conclusions

In summary, the special-designed QMCA preforms have been successfully fabricated via combination of QFCs and MCA. With the enhancement of CNPs, uniformly dispersed nanotubes not only form superior conductive network throughout the preform, but also adhere to QFCs very closely. The 3D CNT networks significantly improve the roughness of fibers' surfaces, and provide more porous channel for PDMS to bond with the cloth. Thus, the QMCA/PDMS composites show both remarkable electrical and mechanical properties. With only 1.6 wt% MWCNTs loading, the electrical conductivity of the laminate can reach 1.67 S cm⁻¹, and remains constant even after 5000 times bending. With the synergistic effect of fibers and nanotubes aerogel, the electrical conductivity retention rate of QMCA/PDMS laminate was nearly 1.7× higher than that of MCA/PDMS at 20% strain. Moreover, at the same MWCNTs concentration, the tensile strength and modulus of the composites are 129.6 MPa and 3.41 GPa respectively, which exhibit an ~ 120 % and 330 % increase than QC/PDMS laminates. Meanwhile, the EMI SE of them can reach around 16 dB in X-band (8-12 GHz) region, which is still an excellent value at such low nanotubes loading. These excellent properties will broaden the potential applications of these brand-new FCs in next-generation devices, like E-skin, robot joints and so on.

Acknowledgements

This work was supported by the National Natural Science Foundation of China (51173043, 21236003, 21322607), the Special Projects for Nanotechnology of Shanghai (11nm0500200), the Basic Research Program of Shanghai (13JC1408100), Program for New Century Excellent Talents in University (NCET-11-0641), the Fundamental Research Funds for the Central Universities.

Notes and references

- ^a Key Laboratory for Ultrafine Materials of Ministry of Education, School of Materials Science and Engineering, East China University of Science and Technology, 130 Meilong Road, Shanghai 200237, China, Email: zlingzi@ecust.edu.cn, czli@ecust.edu.cn; Fax: +86 21 64250624; Tel: +86 21 64250949
- R. F. Service, *Science*, 2003, **301**(5635), 909-911.
 - J. A. Rogers, T. Someya, Y. Huang, *Science*, 2010, **327**(5973), 1603-1607.
 - Y. Li and H. Shimizu, *Macromolecules*, 2009, **42**, 2587-2593.
 - N. Liu, G. Fang, W. Zeng, H. Zhou, H. Long, X. Zhao, *J. Mater. Chem.*, 2012, **22**, 3478-3484.
 - T. Someya, T. Sekitani, S. Iba, Y. Kato, H. Kawaguchi, T. Sakurai, *Proc. Natl. Acad. Sci. USA*, 2004, **101**, 9966.
 - M. Terrones, O. Martin, M. González, J. Pozuelo, B. Serrano, J. C. Cabanelas, S. M. V-Dlaz and J. Baselga, *Adv. Mater.*, 2011, **23**(44), 5302-5310.
 - R. Pelrine, R. Kombluh, G. Kofod, *Adv. Mater.*, 2000, **12**(16), 1223.
 - Y. Li, L. Zhao and H. Shimizu, *Macromol. Rapid. Commun.*, 2011, **32**, 289-294.

- 9 A. B. Kaiser and V. Skákalová, *Chem. Soc. Rev.*, 2011, **40**, 3786-3801.
- 10 C. Luo, X. Zuo, L. Wang, E. Wang, S. Song, J. Wang, J. Wang, C. Fan and Y. Cao, *Nano Lett.*, 2008, **8(12)**, 4454-4458.
- 11 J. Chen, Y. Liu, A. I. Minett, C. Lynam, J. Wang and G. G. Wallace, *Chem. Mater.*, 2007, **19(15)**, 3595-3597.
- 12 M. Chen, T. Tao, L. Zhang, W. Gao and C. Li, *Chem. Commun.*, 2013, **49**, 1612-1614.
- 13 M. A. Worsley, S. O. Kucheyav, J. D. Kuntz, A. V. Hamza, J. H. Satcher, Jr. and T. F. Baumann, *J. Mater. Chem.*, 2009, **19**, 3370-3372.
- 14 T. Someya, T. Sekitani, S. Iba, Y. Kato, H. Kawaguchi, T. Sakurai, *Proc. Natl. Acad. Sci. USA*, 2004, **101**, 9966-9970.
- 15 Z. Chen, C. Xu, C. Ma, W. Ren, and H. -M. Cheng, *Adv. Mater.*, 2013, **25(9)**, 1296-1300.
- 16 Y. Yang, M. C. Gupta, K. L. Dudley, R. W. Lawrence, *Nano Lett.* 2005, **5(11)**, 2131-2134.
- 17 M. Mahmoodi, M. Arjmand, U. Sundararaj and S. Park, *Carbon*, 2012, **50**, 1455-1464.
- 18 R. M. Bagwell, J. M. McManaman and R. C. Wetherhold, *Compos. Sci. Technol.*, 2006, **66(3-4)**, 522-530.
- 19 C. J. von Klemperer and D. Maharaj, *Compos. Struct.*, 2009, **91**, 467-472.
- 20 M. A. Worsley, P. J. Pauzauskie, S. O. Kucheyev, J. M. Zaug, A. V. Hamza, J. H. Satcher Jr. and T. F. Baumann, *Acta Materialia* 2009, **57(17)**, 5131-5136.
- 21 L. Jin, L. Zhang, D. Su and C. Li, *Ind. Eng. Chem. Res.*, 2012, **51(13)**, 4927-4933.
- 22 A. M. D.- Pascual, B. Ashrafi, M. Naffakh, J. M. G.- Domínguez, A. Johnston, B. Simard, M. T. Martínez and M. A. G.- Fatou, *Carbon*, 2011, **49(8)**, 2817-2833.
- 23 Q. Peng, X. He, Y. Li, C. Wang, R. Wang, P. Hu, Y. Yan and T. Sritharan, *J. Mater. Chem.*, 2012, **22**, 5928-5931.
- 24 D. -H. Kim and J. A. Rogers, *Adv. Mater.* 2008, **20(24)**, 4887-4892.
- 25 B. Hu, D. Li, P. Manandharm, Q. Fan, D. Kasilingam and P. Calvert, *J. Mater. Chem.*, 2012, **22**, 1598-1605.
- 26 T. Sekitani, Y. Noguchi, K. Hata, T. Fukushima, T. Aida and T. Someya, *Science* 2008, **321(5895)**, 1468-1472.
- 27 U. Basuli, S. Chattopadhyay, C. Nah and T. K. Chaki, *Polym. Compos.*, 2012, **33(6)**, 897-903.
- 28 M. Arjmand, M. Mahmoodi, G. A. Gelves, S. Park and U. Sundararaj, *Carbon*, 2011, **49**, 3430-3440.
- 29 D. D. L. Chung, *Composite materials: functional materials for modern technologies*. New York: Springer; 2003, p. 91-99.
- 30 M. H. Al-Salah and U. Sundararaj, *Carbon*, 2009, **47**, 1738-1746.
- 31 J. M. Thomassin, C. Pagnouille, L. Bednarz, I. Huynen, R. Jerome and C. Detrembleur, *J. Mater. Chem.*, 2008, **18**, 792.
- 32 N. Li, Y. Huang, F. Du, X. B. He, X. Lin, H. J. Gao, Y. F. Ma, F. F. Li, Y. S. Chen, P. C. Eklund, *Nano Lett.*, 2006, **6**, 1141.
- 33 M. H. Al-Saleh, W. H. Saadeh and U. Sundararaj, *carbon*, 2013, **60**, 146-156.
- 34 U. Basuli, S. Chattopadhyay, C. Nah, TK. Chaki, *Polym. Compos.*, 2012, **33(6)**, 897-903.
- 35 V. Eswaraiah, V. Sankaranarayanan and S. Ramaprabhu, *Macromol. Mater. Eng.* 2011, **296**, 894-898.
- 36 D. D. L. Chung, *Carbon*, 2001, **39**, 279-285.
- 37 I. Balberg, *Phys. Rev. Lett.* 1987, **59(12)**, 1305-1308.